
Conditional Perceptual Quality Preserving Image Compression

Tongda Xu

Air, Tsinghua University
x.tongda@nyu.edu

Qian Zhang

Air, Tsinghua University
zhangqian@stu.xjtu.edu.cn

Yanghao Li

Air, Tsinghua University
liyangha18@mails.tsinghua.edu.cn

Dailan He

The Chinese University of Hong Kong
hedailan@sensetime.com

Zhe Wang

Air, Tsinghua University
wangzhe@air.tsinghua.edu.cn

Yuanyuan Wang

Sensetime Research
wangyuanyuan@sensetime.com

Hongwei Qin

Sensetime Research
qinhongwei@sensetime.com

Yan Wang

Air, Tsinghua University
wangyan@air.tsinghua.edu.cn

Jingjing Liu

Air, Tsinghua University
JJLiu@air.tsinghua.edu.cn

Ya-Qin Zhang

Air, Tsinghua University
zhangyaqin@air.tsinghua.edu.cn

Abstract

We propose conditional perceptual quality, an extension of the perceptual quality defined in Blau and Michaeli [2018], by conditioning it on user defined information. Specifically, we extend the original perceptual quality $d(p_X, p_{\hat{X}})$ to the conditional perceptual quality $d(p_{X|Y}, p_{\hat{X}|Y})$, where X is the original image, \hat{X} is the reconstructed, Y is side information defined by user and $d(\cdot, \cdot)$ is divergence. We show that conditional perceptual quality has similar theoretical properties as rate-distortion-perception trade-off [Blau and Michaeli, 2019]. Based on these theoretical results, we propose an optimal framework for conditional perceptual quality preserving compression. Experimental results show that our codec successfully maintains high perceptual quality and semantic quality at all bitrate. Besides, by providing a lowerbound of common randomness required, we settle the previous arguments on whether randomness should be incorporated into generator for (conditional) perceptual quality compression. The source code is provided in supplementary material.

1 Introduction

How to optimize image compression algorithms to preserve perceptual quality is a fundamental problem. As mean square error (MSE) leads to blurry results, various loss functions are designed including SSIM [Wang et al., 2004] and LPIPS [Zhang et al., 2018]. In 2018, Blau and Michaeli [2018] formalize perceptual quality as the divergence of original image distribution and distorted

image distribution. Specifically, given an original image X and distorted image \hat{X} , they evaluate perceptual quality as $d(p_X, p_{\hat{X}})$, where $d(\cdot, \cdot)$ is the divergence. Later, their theory is developed into rate-distortion-perception trade-off [Blau and Michaeli, 2019]. Since then, rate-distortion-perception trade-off has become the theoretical cornerstone for perceptual quality preserving image compression [Agustsson et al., 2019, Mentzer et al., 2020, Agustsson et al., 2022], which also provides a theoretical justification of previous codecs using generative adversarial network [Rippel and Bourdev, 2017, Tschannen et al., 2018].

However, perceptual quality preserving compression alone is not enough. Consider we have a codec for MNIST dataset [LeCun and Cortes, 2005]. At low bitrate, a perceptual quality preserving codec might decode an image of "7" from an original image of "3" (See Fig. 4). Though the decoded image of "7" has perfect perceptual quality, the digit is incorrect. Another example is in Tschannen et al. [2018], where a perceptual quality preserving codec might compress the image of one bedroom into another with completely different layout. Though the decoded bedroom has perfect perceptual quality, the layout of bedroom is wrongly depicted.

In both cases, there is specific side information that we want to keep in the original images. Let's denote this information as Y . For the MNIST case, Y is the digit. And for the bedroom case, Y is the layout. In both bases, the perceptual quality is perfect, and the divergence between original image and distorted image $d(p_X, p_{\hat{X}}) = 0$. However, the divergence between the images' posterior on Y is obviously different, indicating a large divergence $d(p_{X|Y}, p_{\hat{X}|Y})$ between conditional distributions.

In this paper, we propose conditional perceptual quality, which considers the divergence between conditional distributions $d(p_{X|Y}, p_{\hat{X}|Y})$ instead of $d(p_X, p_{\hat{X}})$. We show that such conditional extension shares similar desirable theoretical properties to rate-distortion-perception trade-off [Blau and Michaeli, 2019]. Based on those theoretical properties, we propose an optimal coding framework to achieve perfect conditional perceptual quality. We empirically show that our coding framework can achieve high perceptual quality and semantic quality at all bitrate with bounded distortion. And it smoothly interpolates the high-to-low distortion as bitrate increases. Besides, we settle the argument on whether noise should be incorporated into decoder for perceptual quality preserving compression, by proving a lowerbound of noise dimensions required for different rate.

2 Preliminaries

2.1 Rate Distortion Theory

Consider the concatenation of n i.i.d. source images $X^n = \{X_1, \dots, X_n\}$ and an encoder $f^n(\cdot)$, we encode X^n into an index $M^n \in \{1, \dots, 2^{nR^n}\}$ with nR^n bits. Specifically, $R^n = \log |\hat{\mathcal{X}}^n|/n$, and $|\hat{\mathcal{X}}^n|$ is the size of reconstruction alphabet. With a decoder $g^n(\cdot)$, we can obtain the reconstruction image $\hat{X}^n = g^n(M^n) \in \hat{\mathcal{X}}^n$. As in Cover [1999], we define information rate distortion function as

$$R^I(D) = \min_{p_{\hat{X}|X}} I(X, \hat{X}), \text{ s.t. } \mathbb{E}[\Delta(X, \hat{X})] \leq D, \quad (1)$$

where $\Delta(\cdot, \cdot)$ is distortion and D is the distortion constraint. Rate distortion theorem [Cover, 1999] tells us that when $n \rightarrow \infty$, there exists an encoder-decoder (codec) $f^n(\cdot), g^n(\cdot)$ with $\mathbb{E}[\Delta(X^n, \hat{X}^n)] \leq D$ if $R^n > R^I(D)$, and no codec with $R^n < R^I(D)$.

Now, consider a single source image $X \in \mathcal{X}$ and an encoder $f^0(\cdot)$, we encode X into uniquely decodable code $M^0 = f^0(X)$. With a decoder $g^0(\cdot)$, we can obtain a reconstruction image $\hat{X} = g^0(M^0)$. We denote the expected code length of M^0 as $R^0 = \mathbb{E}[\mathcal{L}(M^0)]$. As in Li and El Gamal [2018], we say (R^0, D) is one-shot achievable if there exists a one-shot codec $f^0(\cdot), g^0(\cdot)$ with rate R^0 , distortion $\mathbb{E}[\Delta(X, \hat{X})] \leq D$. And Li and El Gamal [2018] show that any (R^0, D) with

$$R^0 > R^I(D) + \log(R^I(D) + 1) + 6 \quad (2)$$

is achievable.

2.2 Rate-Distortion-Perception Trade-off

Blau and Michaeli [2018] formalize a metric for perceptual quality as the divergence between two image distributions $d(p_X, p_{\hat{X}})$, where p_X is the distribution for the original image, $p_{\hat{X}}$ is the

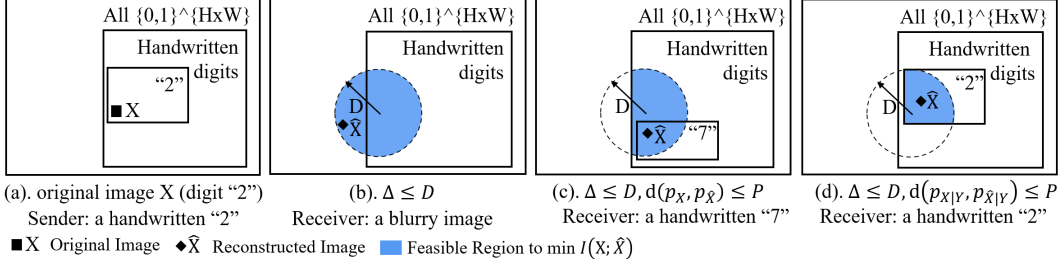


Figure 1: Feasible region of: (a). original image; (b). $R^I(D)$; (c). $R^I(D, P)$; (d). $R_C^I(D, P)$.

distribution of reconstruction image and $d(\cdot, \cdot)$ is the divergence. They show that $d(p_X, p_{\hat{X}})$ is at odds with any distortion $\Delta(X, \hat{X})$ between two specific images. Since then, this definition of perceptual quality has been widely applied to image restoration, super-resolution and compression. Later, Blau and Michaeli [2019] extend the information rate distortion function $R^I(D)$ into rate-distortion-perception function as:

$$R^I(D, P) = \min_{p_{\hat{X}|X}} I(X, \hat{X}), s.t. \mathbb{E}[\Delta(X, \hat{X})] \leq D, d(p_X, p_{\hat{X}}) \leq P, \quad (3)$$

where P is the constraint on divergence. The fundamental properties of $R^I(D, P)$, such as monotonicity, convexity, achievability and converse, and one-shot achievability, are proven by Blau and Michaeli [2019], Theis and Wagner [2021], Zhang et al. [2021] in analogous to rate distortion. Beyond them, more useful properties are also shown:

Theorem 1. When distortion $\Delta(\cdot, \cdot)$ is MSE:

- [Blau and Michaeli, 2019] $R^I(D, 0) \leq R^I(\frac{1}{2}D, \infty) = R^I(\frac{1}{2}D)$;
- [Yan et al., 2021] Given an optimal one-shot codec $f^0(\cdot), g_1^0(\cdot)$ with code M^0 , reconstruction \hat{X} and distortion $\mathbb{E}[\Delta(X, \hat{X})] \leq D/2$, there exists an optimal perceptual decoder $g_2(\cdot)$, with $p_{\hat{X}|M^0} = p_{X|M^0}$, $d(p_X, p_{\hat{X}}) = 0$, $\mathbb{E}[\Delta(X, \hat{X})] \leq D$;

Prior to Theorem. 1, we only know that achieving perfect perceptual quality increases MSE [Tschanen et al., 2018], and there are arguments on whether we should enable the gradient of encoder while training perceptual decoder [Rippel and Bourdev, 2017, Mentzer et al., 2020]. Theorem. 1.1 and Theorem. 1.2 show that we can achieve perfect conditional perceptual quality by first training an MSE codec and then a perceptual decoder, and the cost is at most doubling MSE.

3 Conditional Perceptual Quality Preserving Image Compression

3.1 Rate-Distortion-Conditional Perception Trade-off

We extend the perceptual quality defined by Blau and Michaeli [2018] by considering the divergence between the posteriors of images $d(p_{X|Y}, p_{\hat{X}|Y})$, where Y is the user-defined side information. We name it ‘conditional perceptual quality’. For now we assume Y is shared across encoder and decoder and ignore its bitrate. Later in Theorem. 3, we will show the overhead of this assumption is no more than 2 bits. Similar to rate-distortion-perception function, we define rate-distortion-conditional perception function as:

$$R_C^I(D, P) = \min_{p_{\hat{X}|X, Y}} I(X; \hat{X}|Y), s.t. \mathbb{E}[\Delta(X, \hat{X})|Y] \leq D, d(p_{X|Y}, p_{\hat{X}|Y}) \leq P. \quad (4)$$

To better understand the relationship between $R^I(D)$, $R^I(D, P)$, $R_C^I(D, P)$ and why the conditional perceptual quality makes sense, we revisit the MNIST example. Consider the sender has an image of digit "2" X to send, and all $R^I(D)$, $R^I(D, P)$, $R_C^I(D, P)$ minimize rate $I(X; \hat{X})$ within their feasible region. For $R^I(D)$, the feasible region is a sphere (Fig. 1.(b)) and not all images within it are handwritten digits. It is likely that \hat{X} is a blurry image. On the other hand, constraining perceptual quality $d(p_X, p_{\hat{X}}) \leq P$ makes the feasible region an intersection of all handwritten digits

and the sphere (Fig. 1.(c)). For $R^I(D, P)$, all possible \hat{X} s are handwritten images, but \hat{X} might have different digits. Now consider constraining the conditional perceptual quality $d(p_{X|Y}, p_{\hat{X}|Y}) \leq P$, then the feasible region becomes an intersection of all handwritten "2" and sphere (Fig. 1.(d)). Then for $R_C^I(D, P)$, all possible \hat{X} can be recognized as a handwritten "2" by the receiver.

Now we show that $R_C^I(D, P)$ shares similar theoretical property as $R^I(D, P)$:

Theorem 2. $R_C^I(D, P)$ shares similar fundamental property to $R^I(D, P)$:

1. (monotonicity and convexity) $R_C^I(D, P)$ is monotonously non-increasing in D, P . And when $d(\cdot, \cdot)$ is convex in its second argument, $R_C^I(D, P)$ is convex.
2. (one-shot achievability) There exists a one-shot codec $f^0(\cdot, Y), g^0(\cdot, Y)$ that satisfies $\mathbb{E}[\Delta(X, \hat{X})|Y] \leq D, d(p_{X|Y}, p_{\hat{X}|Y}) \leq P$ if $R^0 > R_C^I(D, P) + \log(R_C^I(D, P) + 1) + 5$;
3. (achievability and converse) When $n \rightarrow \infty$, there exists a codec $f^n(\cdot, Y), g^n(\cdot, Y)$ that satisfies $\mathbb{E}[\Delta(X^n, \hat{X}^n)|Y] \leq D, d(p_{X|Y}, p_{\hat{X}|Y}) \leq P$ if $R^n > R_C^I(D, P)$ and no codec with $R^n < R_C^I(D, P)$;
4. Perfect conditional perceptual quality leads to perfect perceptual quality.

Furthermore, when distortion $\Delta(\cdot, \cdot)$ is MSE:

5. $R_C^I(D, 0) \leq R_C^I(\frac{1}{2}D, \infty)$;
6. Given an optimal one-shot codec $f^0(\cdot, Y), g_1^0(\cdot, Y)$ with code M^0 , reconstruction \hat{X} and distortion $\mathbb{E}[\Delta(X, \hat{X})|Y] \leq D/2$, there exists an optimal perceptual decoder $g_2(\cdot, Y)$ with $p_{\hat{X}|M^0, Y} = p_{X|M^0, Y}, d(p_{X|Y}, p_{\hat{X}|Y}) = 0, \mathbb{E}[\Delta(X, \hat{X})|Y] \leq D$;

Theorem. 2 provides bound and guideline for conditional perceptual quality preserving codec. More specifically, Theorem. 2.5, Theorem. 2.6 show that we can achieve perfect conditional perceptual quality by training first an MSE codec and then a conditional perceptual decoder, and the cost is at most doubling MSE.

3.2 Conditional Perceptual Quality Preserving Image Compression

In previous section, we assume Y is shared across encoder and decoder, and we define $R_C^I(D, P)$ without Y 's bitrate. Now as we are designing practical zero-shot codec, we take the bitrate of Y into consideration. Consider the following coding framework:

1. We encode Y losslessly with expected code length R_Y and share it with decoder;
2. We generate the code $M = f(X, Y)$ and encode M under the condition of Y with expected code length R_M ;
3. The decoder first decodes Y and then with Y it decodes M , and with M it decodes $\hat{X} = g(M, Y)$.

The total expected code length is $R_Y + R_M$. We show that under some mild assumptions, the above coding framework is at most 2 bits from optimal.

Theorem 3. Assume $d(p_{X|Y}, p_{\hat{X}|Y}) = 0$ and Y is deterministic of X , for any codec with total expected code length R and code M , there exists another codec that has the same code M following the above framework with Y encoded losslessly, whose total expected code length $R_M + R_Y \leq R + 2$.

In practice, even for MSE optimized codec with $d(p_{X|Y}, p_{\hat{X}|Y})$ constraint $P = \infty$, the performance decay of the above coding framework is small, as the net bitrate of Y is usually small. By far, we have shown that the above coding scheme is at most 2 bits from optimal (Theorem. 3), and the bitstream of MSE codec and conditional perceptual codec can be shared (Theorem. 2.5). Then, we can extend the perceptual quality preserving codec [Yan et al., 2021] to conditional perceptual quality preserving codec, by encoding Y losslessly and adding a conditional entropy model for code M .

Specifically, for perceptual quality preserving codec (Fig. 2.(a)), Yan et al. [2021] propose the following optimization framework:

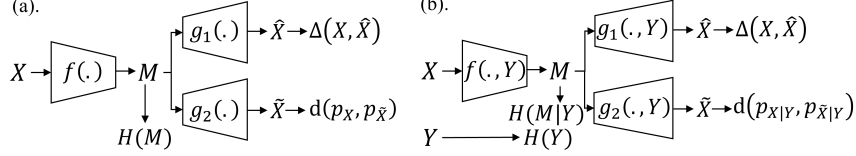


Figure 2: (a). The perceptual quality preserving framework by Yan et al. [2021]. (b). The conditional perceptual quality preserving framework by us.

1. They first optimize an MSE codec $f(\cdot), g_1(\cdot)$ using rate distortion loss $\mathbb{E}[H(M) + \lambda\Delta(X, \hat{X})]$, where $M = f(X)$, $\hat{X} = g_1(M)$, λ is the Lagrangian multiplier controlling rate-distortion trade-off, and $H(M)$ is the entropy of code M ;
2. Then they optimize a perceptual quality preserving decoder $g_2(\cdot)$ with $d(p_{X|M}, p_{\tilde{X}|M}) = 0$ constraint implemented by a conditional generative model.

Theorem. 1.2 shows that ideally this leads to $d(p_X, p_{\tilde{X}}) = 0$ and $\mathbb{E}[\Delta(X, \tilde{X})] \leq 2\mathbb{E}[\Delta(X, \hat{X})]$.

Similarly, for conditional perceptual quality preserving codec (Fig. 2.(b)), we combine the proposed optimal conditional perceptual coding framework with the perceptual quality preserving optimization framework, and propose the following optimization framework:

1. We encode Y losslessly and share it with the decoder with rate close to $H(Y)$.
2. We first optimize an MSE codec $f(\cdot, Y), g_1(\cdot, Y)$ using rate distortion loss $\mathbb{E}[H(M|Y) + \lambda\Delta(X, \hat{X})]$.
3. We then optimize a conditional perceptual quality preserving decoder $g_2(\cdot, Y)$, with $d(p_{X|M,Y}, p_{\tilde{X}|M,Y}) = 0$ constraint implemented by a conditional generative model.

Theorem. 2.5 shows that ideally this leads to $d(p_{X|Y}, p_{\tilde{X}|Y}) = 0$ and $\mathbb{E}[\Delta(X, \tilde{X})|Y] \leq 2\mathbb{E}[\Delta(X, \hat{X})|Y]$. And Theorem. 3 guarantees that the resulting codec is at most 2 bits from optimal.

3.3 Common Randomness Lowerbound

Finally, one practical issue that has not been well understood is the random noise W injected at $g_2(\cdot)$ for perfect (conditional) perceptual quality. Previous works in perceptual compression empirically show W is required for low bitrate [Tschannen et al., 2018, Yan et al., 2021], not required for high bitrate [Tschannen et al., 2018, Mentzer et al., 2020, Agustsson et al., 2022], and is beneficial in a tractable example Theis and Agustsson [2021]. To settle those arguments, we quantify the least amount of randomness required to achieve perfect (conditional) perceptual quality for one-shot codec in the next theorem.

Theorem 4. *For one-shot codec, to achieve perfect perceptual quality at rate R^0 , we require a common randomness $W \in \mathcal{W}$ with at least $\log |\mathcal{W}| \geq H(W) \geq H(X) - (R^0 + 1)$. To achieve perfect conditional perceptual quality, we require $\log |\mathcal{W}| \geq H(W) \geq H(X|Y) - (R^0 + 1)$.*

Intuitively, Theorem. 4 tells us that the amount of bitrate reduced by lossy codec is the amount of common randomness required. And this result is aligned with previous empirical results. When bitrate R^0 is high, the required $|\mathcal{W}|$ is small and sometimes can be ignored. When R^0 is low, the required $|\mathcal{W}|$ can be too large to be ignored, and thus becomes necessary.

4 Experiments

4.1 Experiment Setup

For all the experiments, we assume Y is deterministic of X , and our target is perfect conditional perceptual quality, which means $d(p_{X|Y}, p_{\tilde{X}|Y}) = 0$. All the experiments are conducted on a computer with AMD EPYC 7742 64-Core Processor and 8 Nvidia A30 GPU. All the code is

implemented with Python 3.10 and Pytorch 1.13. The dataset, data type of Y , baselines, details of encoder-decoder architecture are specified in each subsections.

Ideally, we evaluate the total bitrate R , distortion $\mathbb{E}[\Delta(X, \hat{X})|Y]$ and divergence $d(p_{X|Y}, p_{\hat{X}|Y})$. The bitrate is evaluated by entropy and implemented via arithmetic coding [Rissanen and Langdon, 1979]. The distortion is MSE. However, there is no direct way to evaluate $d(p_{X|Y}, p_{\hat{X}|Y})$. The common method to approximate the perceptual quality $d(p_X, p_{\hat{X}})$ is Fréchet Inception Distance (FID) $d_F(p_X, p_{\hat{X}})$. Similarly, for Y that is tractable to enumerate, we enumerate each $y_i \in Y$, evaluate prior $p_{Y=y}$, FID $d_F(p_{X|Y=y}, p_{\hat{X}|Y=y})$, and $d_F(p_{X|Y}, p_{\hat{X}|Y}) = \sum p_{Y=y} d_F(p_{X|Y=y}, p_{\hat{X}|Y=y})$ as an approximation to $d(p_{X|Y}, p_{\hat{X}|Y})$. We name this metric as conditional FID (ConFID). In addition, we also use FID to evaluate the perceptual quality $d(p_X, p_{\hat{X}})$, and a pre-trained model to predict Y from \hat{X} to evaluate the accuracy $d(p_{Y|X}, p_{Y|\hat{X}})$. As when both of them are 0, $d(p_{X|Y}, p_{\hat{X}|Y}) = 0$. Thus, combining those two might give us a hint about $d(p_{X|Y}, p_{\hat{X}|Y})$.

4.2 Evaluation on MNIST Dataset

Setup We first evaluate our method on MNIST dataset [LeCun and Cortes, 2005] with Y as the digit. This is the MNIST example we mentioned previously, where the users want perfect perceptual quality with correct digits and minimal rate. The baseline MSE codec and the training details are exactly the same as Yan et al. [2021]. The difference is: we train our MSE codec g_1 with Y available to decoder and entropy model of M ; we train our perceptual decoder g_2 with Y available to decoder and discriminator. And Y is losslessly encoded within log 10 bits. We evaluate the rate, MSE, ConFID, FID and classification accuracy. The digits predicted for accuracy is from a model pre-trained on training dataset (See Appendix. B.1 for details).

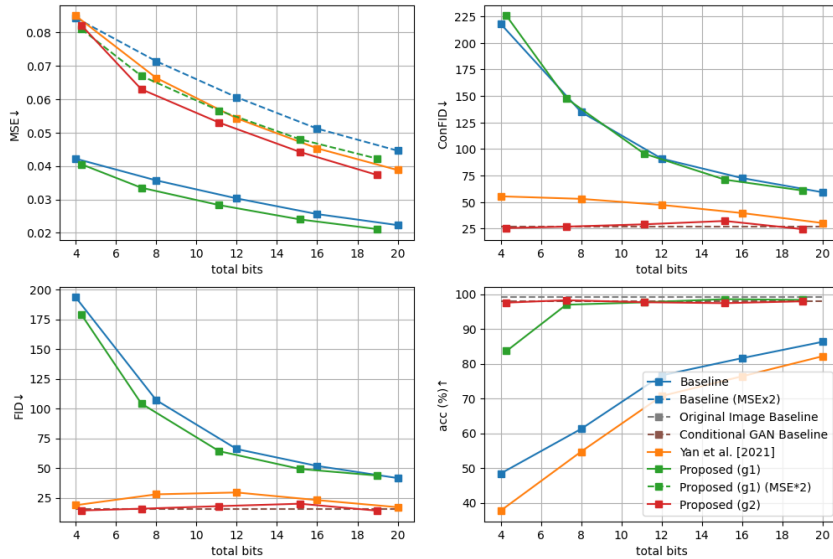


Figure 3: The bitrate-MSE, bitrate-ConFID, bitrate-FID, bitrate-accuracy of different methods.

Table 1: The BD-MSE, BD-ConFID, BD-FID, BD-acc of different methods on MNIST dataset.

| Methods | Constrains | BD-MSE ↓ | BD-ConFID ↓ | BD-FID ↓ | BD-acc ↑ |
|--------------------|--|----------------|---------------|---------------|--------------|
| Baseline | $\mathbb{E}[\Delta] \leq D$ | 0.0000 | 0.00 | 0.00 | 0.00 |
| Yan et al. [2021] | $\mathbb{E}[\Delta] \leq D, p_X = p_{\hat{X}}$ | 0.0229 | -48.99 | -47.67 | -6.81 |
| Proposed (g_1) | $\mathbb{E}[\Delta] \leq D$ | -0.0009 | 9.65 | 3.21 | 29.22 |
| Proposed (g_2) | $\mathbb{E}[\Delta] \leq D, p_{X Y} = p_{\hat{X} Y}$ | 0.0227 | -62.15 | -50.75 | 31.19 |

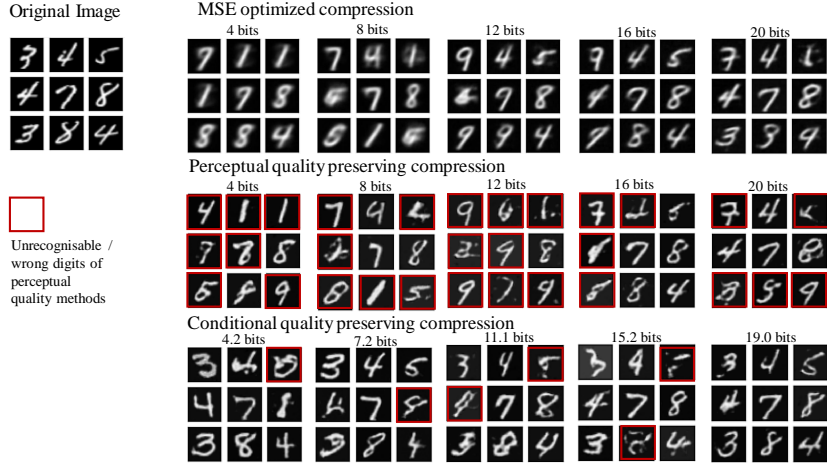


Figure 4: The qualitative results of different methods on MNIST dataset. We mark obvious unrecognisable / wrong digits of two perceptual preserving methods in red.

Quantitative Results We show the rate, distortion in MSE, ConFID, FID and classification accuracy of different methods in Fig. 3 and Tab. 1. It is shown that our framework optimized for MSE (Proposed (g_1)) is on par with the baseline approach in terms of BD-MSE (-0.0009% vs 0.0000%). Surprisingly, our framework optimized for conditional perceptual quality (Proposed (g_2)) slightly outperforms Yan et al. [2021] in terms of BD-MSE and BD-FID (0.0227% vs 0.0229%, -50.75% vs -47.67%). This means that Proposed (g_2) achieves good rate-distortion-perception trade-off. This unexpected result might due to the fact that the digit of an image is an important feature that is more efficient to store than the feature learned by auto-encoder. On the other hand, Proposed (g_2) has significant advantage over all other methods in terms of BD-ConFID (-62.15% vs 0.00%, -48.99%, 9.65%), and significantly outperforms baseline and Yan et al. [2021] in terms of BD-acc (31.19% vs 0.00%, -6.81%). Those results clearly show the advantage of the Proposed (g_2) in terms of rate-distortion-conditional perceptual quality trade-off. In addition, Proposed (g_2)’s MSE lies below the double of Proposed (g_1)’s MSE, which conforms the theoretical results in Theorem. 2.

Qualitative Results We show the qualitative comparison of different methods in Fig. 4. It can be seen that the MSE-optimized image is blurry and un-recognisable at low bitrate. On the other hand, the perceptual preserving [Yan et al., 2021] image is visually pleasing, while it often leads to wrong digits. And our proposed conditional perceptual preserving codec (Proposed (g_2)) leads to visually pleasing image with more accurate digit at the same time.

Distortion-Conditional Perception Trade-off Though Theorem. 2.6 show that it is possible to achieve perfect (conditional) perceptual quality with MSE encoder, it is unclear whether other middle points between $P = 0$ and $P = \infty$ can be achieved with the same bitstream. Existing theoretical results [Zhang et al., 2021, Freirich et al., 2021, Yan et al., 2022] assume $d(\cdot, \cdot)$ to be Wasserstein-2 (W2) distance. This is not very useful for practical codec as W2 does not have a GAN form and requires special tricks to optimize [Korotin et al., 2019].

However, it remains alluring to test the method proposed in [Freirich et al., 2021, Yan et al., 2022] empirically. More specifically, Freirich et al. [2021], Yan et al. [2022] show that when $d(\cdot, \cdot)$ is W2 distance, any perception-distortion trade-off can be achieved by convex combination between MSE optimized image \hat{X} and perfect perceptual quality image \tilde{X} . This requires only 2 decoder and saves users from complicated decoder manipulation [Iwai et al., 2020, Agustsson et al., 2022]. We linearly interpolate the image reconstructed from g_1 and g_2 , and show their MSE-ConFID. The baseline approach is to jointly train the encoder and decoder to minimize $R + \lambda E[\Delta(X, \hat{X})] + \beta d(p_{X|Y}, p_{\hat{X}|Y})$, with D-P trade-off achieved by adjusting β . Fig. 5

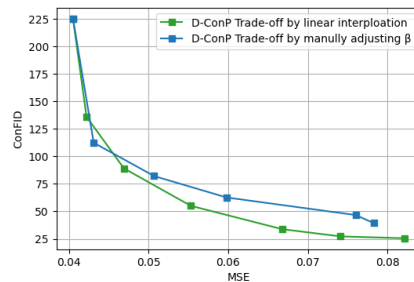


Figure 5: The MSE-ConFID trade-off.

shows that simple linear interpolation of images outperforms direct joint training. All the (D, P) points have very similar bitrate and the details are listed in Appendix. B.2.

Evaluation on Common Randomness Required In addition to the proposed codec, we also verify the correctness of Theorem 4, which is about the lowerbound of common randomness for perfect (conditional) perceptual quality. The details are provided in Appendix. B.4.

4.3 Evaluation on Cityscape Dataset

Setup We evaluate our method on Cityscape dataset [Cordts et al., 2016] with Y as the segmentation map down-sampled by 8. This is similar to the bedroom layout example we mention in previous section, where the users want perfect perceptual quality with roughly correct layout. The baseline MSE codec is Ballé et al. [2018]. For GAN, we adopt the generator and discriminator structure of Sushko et al. [2020]. For perceptual codec Yan et al. [2021], we train GAN unconditionally. For conditional perceptual codec, we train GAN conditioned on Y , which is compressed losslessly by BMF [bmf] into 0.00742 bpp. Different from MNIST, Y is not enumerable and ConfID is not available. Thus, we evaluate the rate, MSE, FID and segmentation mIoU. The segmentation map predicted for mIoU is computed by a model [Yu et al., 2017] pre-trained on Cityscape training dataset (See Appendix. B.1 for details).

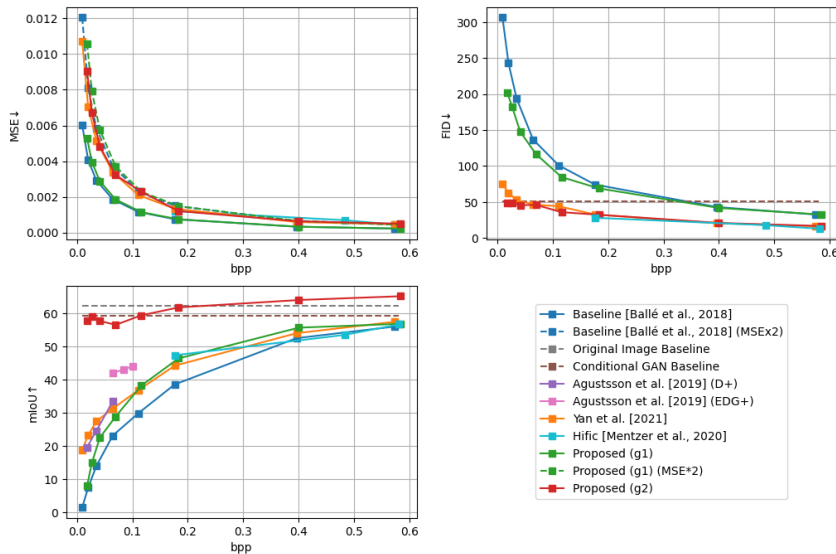


Figure 6: The bitrate-MSE, bitrate-FID, bitrate-mIoU of different methods.

Table 2: The BD-MSE, BD-FID, BD-mIoU of different methods on Cityscape dataset.

| Methods | Constrains | BD-MSE ↓ | BD-FID ↓ | BD-mIoU ↑ |
|--------------------------------|--|----------------|----------------|--------------|
| Baseline [Ballé et al., 2018] | $\mathbb{E}[\Delta] \leq D$ | 0.0000 | 0.00 | 0.00 |
| Agustsson et al. [2019] (D+) | complex | - | - | 11.01 |
| Agustsson et al. [2019] (EDG+) | complex | - | - | 16.89 |
| Hific Mentzer et al. [2020] | complex | 0.0022 | -132.28 | 9.87 |
| Yan et al. [2021] | $\mathbb{E}[\Delta] \leq D, p_X = p_{\hat{X}}$ | 0.0022 | -132.28 | 9.87 |
| Proposed (g_1) | $\mathbb{E}[\Delta] \leq D$ | -0.0004 | -62.64 | 4.97 |
| Proposed (g_2) | $\mathbb{E}[\Delta] \leq D, p_{X Y} = p_{\hat{X} Y}$ | 0.0017 | -167.24 | 40.32 |

Quantitative Results We show the rate, distortion in MSE, FID and segmentation mIoU of different methods in Fig. 6 and Tab. 2. Our framework optimized for MSE (Proposed (g_1)) is on par with the baseline approach in terms of BD-MSE (-0.0004% vs 0.0000%). And again, our framework optimized for conditional perceptual quality (Proposed (g_2)) marginally outperforms Yan et al. [2021] in terms of BD-MSE and BD-FID (0.0017% vs 0.0022%, -167.24% vs -132.28%). On the other

hand, Proposed (g_2) has significant advantage over all other methods in terms of BD-mIoU (40.32% vs 0.00%, 11.01%, 16.89%, 9.87%, 4.97%). In addition, Proposed (g_2)’s MSE lies below the double of Proposed (g_1)’s MSE, which conforms the theoretical results in Theorem. 2.

Qualitative Results We show the qualitative comparison of different methods in Fig. 7. Obviously the MSE-optimized image is blurry and un-recognisable at low bpp. Though the perceptual codec [Yan et al., 2021] is visually pleasing, it generates wrong objects. And our proposed approach leads to visually pleasing image with accurate semantic information at the same time.

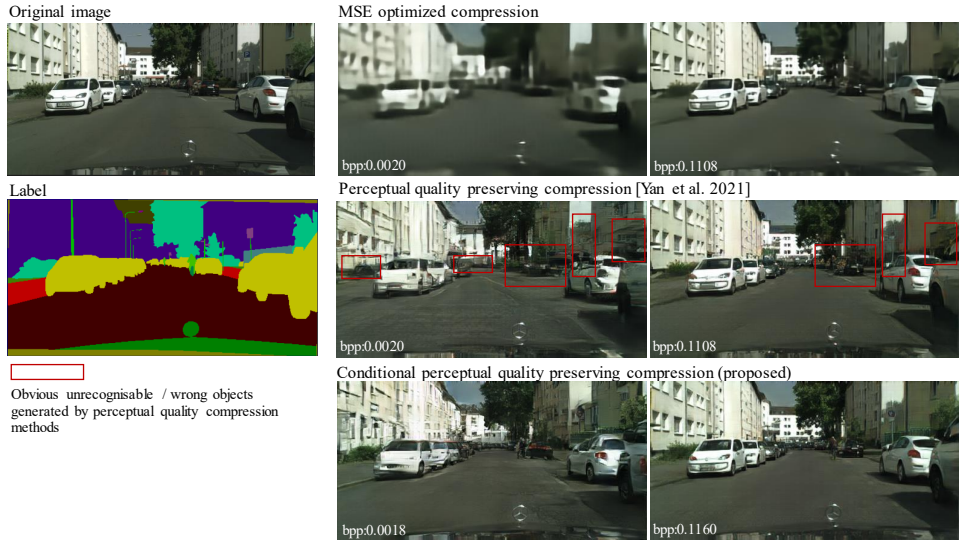


Figure 7: Qualitative comparison of different methods on Cityscape dataset. We mark obvious unrecognisable / wrong objects of two perceptual quality preserving methods in red.

5 Related Work

The perceptual quality by Blau and Michaeli [2018] and rate-distortion-perception trade-off [Blau and Michaeli, 2019] have been well discussed in previous section. Another work related to us is the classification-distortion-perception trade-off [Liu et al., 2019]. It considers Y , the classification label as a separate term while we consider the posterior of image on Y . On the other hand, recent studies in information theory Wagner [2022], Chen et al. [2022] conclude that no deterministic lossy codec exists for strong-sense perfect perceptual quality, which is different from our definition.

The pioneers of perceptual quality preserving image compression[Rippel and Bourdev, 2017, Tschannen et al., 2018] achieve perfect perceptual quality using generative model before perception-distortion trade-off [Blau and Michaeli, 2018]. Later works [Mentzer et al., 2020] improve the usability by incorporating extra distortion constrains. [Zhang et al., 2021, Yan et al., 2021] show that we can achieve any perception-distortion trade-off without changing bitstream. Furthermore, Freirich et al. [2021], Yan et al. [2022] show that perception-distortion trade-off can be achieved by linear interpolation between images, without complicated decoder manipulation [Iwai et al., 2020, Agustsson et al., 2022]. There are other works utilize segmentation map for perceptual quality that resemble the experiment in Section 4.2 [Agustsson et al., 2018, 2019, Duan et al., 2022]. However, they are limited to Y as segmentation map and do not have theoretical optimality.

6 Discussion & Conclusion

One limitation is that the current Y chosen for experiment remains simple. It would be more interesting to see the results when Y is image caption or description, combining the text-to-image models such as DALL-E [Ramesh et al., 2021]. Furthermore, the image resolution and model size

used in this paper is relatively small. It would be more interesting to see the results on large size image and large model.

To conclude, we propose conditional perceptual quality, an extension of perceptual quality proposed by Blau and Michaeli [2018]. We show that it shares similar theoretical properties as rate-distortion-perception trade-off [Blau and Michaeli, 2019]. Based on those properties, we propose an optimal conditional perceptual quality preserving codec. And we empirically show that our codec successfully achieves high perceptual quality and semantic quality at the same time. Furthermore, we settle the argument about the randomness requirement to achieve perfect (conditional) perceptual quality by providing a lowerbound on randomness required.

References

- Bmf 2.01 image codec software. <https://encode.su/threads/2838-BMF-2-01-Fixed-for-FreeArc?highlight=bmf>. Accessed: 2023-03-01.
- E. Agustsson, M. Tschannen, F. Mentzer, R. Timofte, and L. V. Gool. Extreme learned image compression with gans. In *CVPR Workshops*, 2018.
- E. Agustsson, M. Tschannen, F. Mentzer, R. Timofte, and L. V. Gool. Generative adversarial networks for extreme learned image compression. In *Proceedings of the IEEE/CVF International Conference on Computer Vision*, pages 221–231, 2019.
- E. Agustsson, D. C. Minnen, G. Toderici, and F. Mentzer. Multi-realism image compression with a conditional generator. *ArXiv*, abs/2212.13824, 2022.
- J. Ballé, D. Minnen, S. Singh, S. J. Hwang, and N. Johnston. Variational image compression with a scale hyperprior. In *International Conference on Learning Representations*, 2018.
- Y. Blau and T. Michaeli. The perception-distortion tradeoff. In *Proceedings of the IEEE conference on computer vision and pattern recognition*, pages 6228–6237, 2018.
- Y. Blau and T. Michaeli. Rethinking lossy compression: The rate-distortion-perception tradeoff. In *International Conference on Machine Learning*, pages 675–685. PMLR, 2019.
- J. Chen, L. Yu, J. Wang, W. Shi, Y. Ge, and W. Tong. On the rate-distortion-perception function. *IEEE Journal on Selected Areas in Information Theory*, 2022.
- M. Cordts, M. Omran, S. Ramos, T. Rehfeld, M. Enzweiler, R. Benenson, U. Franke, S. Roth, and B. Schiele. The cityscapes dataset for semantic urban scene understanding. *2016 IEEE Conference on Computer Vision and Pattern Recognition (CVPR)*, pages 3213–3223, 2016.
- T. M. Cover. *Elements of information theory*. John Wiley & Sons, 1999.
- S. Duan, H. Chen, and J. Gu. Jpd-se: High-level semantics for joint perception-distortion enhancement in image compression. *IEEE Transactions on Image Processing*, 31:4405–4416, 2022.
- D. Freirich, T. Michaeli, and R. Meir. A theory of the distortion-perception tradeoff in wasserstein space. *ArXiv*, abs/2107.02555, 2021.
- K. He, X. Zhang, S. Ren, and J. Sun. Deep residual learning for image recognition. *2016 IEEE Conference on Computer Vision and Pattern Recognition (CVPR)*, pages 770–778, 2015.
- G. Hinton, N. Srivastava, and K. Swersky. Neural networks for machine learning lecture 6a overview of mini-batch gradient descent. *Cited on*, 14(8):2, 2012.
- S. Iwai, T. Miyazaki, Y. Sugaya, and S. Omachi. Fidelity-controllable extreme image compression with generative adversarial networks. *2020 25th International Conference on Pattern Recognition (ICPR)*, pages 8235–8242, 2020.
- D. P. Kingma and J. Ba. Adam: A method for stochastic optimization. *CoRR*, abs/1412.6980, 2014.
- A. Korotin, V. Egiazarian, A. Asadulaev, A. Safin, and E. Burnaev. Wasserstein-2 generative networks. *arXiv preprint arXiv:1909.13082*, 2019.

- Y. LeCun and C. Cortes. The mnist database of handwritten digits. 2005.
- C. T. Li and A. El Gamal. Strong functional representation lemma and applications to coding theorems. *IEEE Transactions on Information Theory*, 64(11):6967–6978, 2018.
- D. Liu, H. Zhang, and Z. Xiong. On the classification-distortion-perception tradeoff. *Advances in Neural Information Processing Systems*, 32, 2019.
- F. Mentzer, G. Toderici, M. Tschannen, and E. Agustsson. High-fidelity generative image compression. *ArXiv*, abs/2006.09965, 2020.
- T. Park, M.-Y. Liu, T.-C. Wang, and J.-Y. Zhu. Semantic image synthesis with spatially-adaptive normalization. In *Proceedings of the IEEE/CVF conference on computer vision and pattern recognition*, pages 2337–2346, 2019.
- N. Qian. On the momentum term in gradient descent learning algorithms. *Neural networks : the official journal of the International Neural Network Society*, 12 1:145–151, 1999.
- A. Ramesh, M. Pavlov, G. Goh, S. Gray, C. Voss, A. Radford, M. Chen, and I. Sutskever. Zero-shot text-to-image generation. In M. Meila and T. Zhang, editors, *Proceedings of the 38th International Conference on Machine Learning*, volume 139 of *Proceedings of Machine Learning Research*, pages 8821–8831. PMLR, 18–24 Jul 2021. URL <https://proceedings.mlr.press/v139/ramesh21a.html>.
- O. Rippel and L. D. Bourdev. Real-time adaptive image compression. In *International Conference on Machine Learning*, 2017.
- J. Rissanen and G. G. Langdon. Arithmetic coding. *IBM Journal of research and development*, 23(2): 149–162, 1979.
- V. Sushko, E. Schönfeld, D. Zhang, J. Gall, B. Schiele, and A. Khoreva. You only need adversarial supervision for semantic image synthesis. *ArXiv*, abs/2012.04781, 2020.
- L. Theis and E. Agustsson. On the advantages of stochastic encoders. *arXiv preprint arXiv:2102.09270*, 2021.
- L. Theis and A. B. Wagner. A coding theorem for the rate-distortion-perception function. *arXiv preprint arXiv:2104.13662*, 2021.
- J. Townsend, T. Bird, and D. Barber. Practical lossless compression with latent variables using bits back coding. In *International Conference on Learning Representations*, 2018.
- M. Tschannen, E. Agustsson, and M. Lucic. Deep generative models for distribution-preserving lossy compression. *Advances in neural information processing systems*, 31, 2018.
- A. B. Wagner. The rate-distortion-perception tradeoff: The role of common randomness. *arXiv preprint arXiv:2202.04147*, 2022.
- Z. Wang, A. C. Bovik, H. R. Sheikh, and E. P. Simoncelli. Image quality assessment: from error visibility to structural similarity. *IEEE transactions on image processing*, 13(4):600–612, 2004.
- Z. Yan, F. Wen, R. Ying, C. Ma, and P. Liu. On perceptual lossy compression: The cost of perceptual reconstruction and an optimal training framework. *ArXiv*, abs/2106.02782, 2021.
- Z. Yan, F. Wen, and P.-Y. Liu. Optimally controllable perceptual lossy compression. *ArXiv*, abs/2206.10082, 2022.
- F. Yu, V. Koltun, and T. Funkhouser. Dilated residual networks. In *Computer Vision and Pattern Recognition (CVPR)*, 2017.
- G. Zhang, J. Qian, J. Chen, and A. Khisti. Universal rate-distortion-perception representations for lossy compression. *ArXiv*, abs/2106.10311, 2021.
- R. Zhang, P. Isola, A. A. Efros, E. Shechtman, and O. Wang. The unreasonable effectiveness of deep features as a perceptual metric. In *Proceedings of the IEEE conference on computer vision and pattern recognition*, pages 586–595, 2018.

A Proof of Main Results

In this section we give the the proof of main theoretical results.

Theorem 2.1. (*monotonicity and convexity*) $R_C^I(D, P)$ is monotonously non-increasing in D, P . And when $d(\cdot, \cdot)$ is convex in its second argument, $R_C^I(D, P)$ is convex.

Proof. The proof of monotonicity and convexity largely follows Blau and Michaeli [2019].

The feasible region for $p(\hat{X}|X, Y)$ increases as D, P increases. Therefore for $D_0 \leq D_1, P_0 \leq P_1$, any feasible $p(\hat{X}|X, Y)$ for D_0, P_0 is also feasible for D_1, P_1 . And therefore, $R_C^I(D, P)$ is non-increasing in D, P .

To show convexity of $R_C^I(D, P)$, we need to show for any convex combination we have:

$$R_C^I(\lambda D_1 + (1 - \lambda)D_2, \lambda P_1 + (1 - \lambda)P_2) \leq \lambda R_C^I(D_1, P_1) + (1 - \lambda)R_C^I(D_2, P_2) \quad (5)$$

We prove this by constructing $p_{\hat{X}_\lambda|X, Y} = \lambda p_{\hat{X}_1|X, Y} + (1 - \lambda)p_{\hat{X}_2|X, Y}$, where $p_{\hat{X}_1|X, Y}, p_{\hat{X}_2|X, Y}$ are optimal solution to $R_C^I(D_1, P_1), R_C^I(D_2, P_2)$.

Consider the convex combination of mutual information. As $I(X; \hat{X})$ is convex in $p_{\hat{X}|X}$, we have:

$$I(X; \hat{X}_\lambda|Y) \leq \lambda I(X; \hat{X}_1|Y) + (1 - \lambda)I(X; \hat{X}_2|Y) \quad (6)$$

Consider the convex combination of $d(p_{X|Y}, p_{\hat{X}_1|Y}) \leq P_1, d(p_{X|Y}, p_{\hat{X}_2|Y}) \leq P_2$, as $d(\cdot, \cdot)$ is convex in second argument, we have:

$$\begin{aligned} d(p_{X|Y}, p_{\hat{X}_\lambda|Y}) &\leq \lambda d(p_{X|Y}, p_{\hat{X}_1|Y}) + (1 - \lambda)d(p_{X|Y}, p_{\hat{X}_2|Y}) \\ &\leq \lambda P_1 + (1 - \lambda)P_2 \end{aligned} \quad (7)$$

Similarly, as the distortion is a linear function in distribution:

$$\begin{aligned} \mathbb{E}[\Delta(X, \hat{X}_\lambda)|Y] &= \lambda \mathbb{E}[\Delta(X, \hat{X}_1)|Y] + (1 - \lambda)\mathbb{E}[\Delta(X, \hat{X}_2)|Y] \\ &\leq \lambda D_1 + (1 - \lambda)D_2 \end{aligned} \quad (8)$$

Then by definition of $R_C^I(D, P)$, $p_{\hat{X}_\lambda|X, Y}$ is feasible to $R_C^I(\lambda D_1 + (1 - \lambda)D_2, \lambda P_1 + (1 - \lambda)P_2)$, and we have:

$$\begin{aligned} R_C^I(\lambda D_1 + (1 - \lambda)D_2, \lambda P_1 + (1 - \lambda)P_2) &\leq I(X; \hat{X}_\lambda|Y) \\ &\leq \lambda I(X; \hat{X}_1|Y) + (1 - \lambda)I(X; \hat{X}_2|Y) \\ &= \lambda R_C^I(D_1, P_1) + (1 - \lambda)R_C^I(D_2, P_2) \end{aligned} \quad (9)$$

And this completes the proof. \square

Theorem 2.2. (*one-shot achievability*) There exists a one-shot codec $f^0(\cdot, Y), g^0(\cdot, Y)$ that satisfies $\mathbb{E}[\Delta(X, \hat{X})|Y] \leq D, d(p_{X|Y}, p_{\hat{X}|Y}) \leq P$ if $R^0 > R_C^I(D, P) + \log(R_C^I(D, P) + 1) + 5$;

Proof. The proof of Theorem 2.2 and 2.3 is based on the conditional extension of strong functional representation lemma (SFRL) [Li and El Gamal, 2018]. The general framework follows the channel simulation proof by Li and El Gamal [2018] and achievability proof by Theis and Wagner [2021]. As the randomness is presented and we can not simply use joint asymptotic equipartition property [Cover, 1999].

By definition of $R_C^I(D, P)$, $\forall \epsilon > 0$, there exist a $p(\hat{X}|X, Y)$ that satisfies the constrains $\mathbb{E}[\Delta(X, \hat{X})|Y] \leq D, d(p_{X|Y}, p_{\hat{X}|Y}) \leq P$, and:

$$I(X; \hat{X}|Y) \leq R_C^I(D, P) + \epsilon \quad (10)$$

By conditional extension of SFRL [Li and El Gamal, 2018], there exist a $Z \perp (X, Y)$ and can represent $\hat{X} = q(X, Y, Z)$, where $q(\cdot, \cdot, \cdot)$ is the quantization mapping, and

$$H(\hat{X}|Z, Y) \leq I(X; \hat{X}|Y) + \log(I(X; \hat{X}|Y) + 1) + 4 \quad (11)$$

We assume the encoder and decoder share an unlimited randomness W . Let $Z = W$ be the shared randomness, upon observing X , the encoder side compute $\hat{X} = q(X, Y, Z)$ and encode \hat{X} under the condition of Y and Z . Then from Kraft inequality [Cover, 1999], there exist a codec that can encode \hat{X} into uniquely decodable bitstream M . Now the total expected code length:

$$\begin{aligned}
R^0 &= \mathbb{E}[\mathcal{L}(M)] \\
&\leq H(\hat{X}|Y, Z) + 1 \\
&\leq I(X; \hat{X}|Y) + \log(I(X; \hat{X}|Y) + 1) + 5 \\
&\leq R_C^I(D, P) + \log(R_C^I(D, P) + 1 + \epsilon) + 5 + \epsilon \\
&\leq R_C^I(D, P) + \log(R_C^I(D, P) + 1) + 5 + 2\epsilon
\end{aligned} \tag{12}$$

And this completes the proof. \square

Theorem 2.3. (achievability and converse) *When $n \rightarrow \infty$, there exists a codec $f^n(\cdot, Y), g^n(\cdot, Y)$ that satisfies $\mathbb{E}[\Delta(X^n, \hat{X}^n)|Y] \leq D, d(p_{X|Y}, p_{\hat{X}|Y}) \leq P$ if $R^n < R_C^I(D, P)$ and no codec with $R^n < R_C^I(D, P)$;*

Proof. We first proof the achievability.

By definition of $R_C^I(D, P)$, $\forall \epsilon > 0$, there exist a $p(\hat{X}|X, Y)$ that satisfies the constrains $\mathbb{E}[\Delta(X, \hat{X})|Y] \leq D, d(p_{X|Y}, p_{\hat{X}|Y}) \leq P$, and:

$$I(X; \hat{X}|Y) \leq R_C^I(D, P) + \epsilon_1 \tag{13}$$

As the proof of Theorem 2.2, we have a shared randomness Z that satisfies:

$$\begin{aligned}
\frac{1}{n}H(\hat{X}^n|Y^n, Z) &\leq \frac{1}{n}(I(X^n; \hat{X}^n|Y^n) + \log(I(X^n; \hat{X}^n|Y^n) + 1) + 4) \\
&= I(X; \hat{X}|Y) + \frac{1}{n}(\log(nI(X; \hat{X}|Y) + 1) + 4) \\
&\leq R_C^I(D, P) + \frac{1}{n}(\log(nR_C^I(D, P) + 2) + 5)
\end{aligned} \tag{14}$$

Then from the theory of typical set [Cover, 1999], we can construct a codebook with size $2^{H(\hat{X}^n|Y^n) + \epsilon_2}$, which means that we can achieve a rate of $R_C^I(D, P) + \epsilon_3$. And this completes the proof of achievability.

The proof of converse is relatively simple. It closely follows the proof of converse of rate distortion by Cover [1999]:

$$\begin{aligned}
nR^n &\geq H(f^n(X^n)|Y) \\
&\geq I(X^n; f^n(X^n)|Y) \\
&\stackrel{(a)}{\geq} I(X^n; \hat{X}^n|Y) \\
&= H(X^n|Y) - H(X^n|\hat{X}^n, Y) \\
&\geq \sum_{i=1}^n (H(X_i|Y) - H(X_i|\hat{X}_i, Y)) \\
&= \sum_{i=1}^n I(X_i; \hat{X}_i|Y) \\
&\stackrel{(b)}{\geq} \sum_{i=1}^n R_C^I(\mathbb{E}[\Delta(X_i, \hat{X}_i)|Y], d(p_{X_i|Y}, p_{\hat{X}_i|Y})) \\
&\stackrel{(c)}{\geq} nR_C^I(\mathbb{E}[\sum_{i=1}^n \Delta(X_i, \hat{X}_i)|Y], \sum_{i=1}^n d(p_{X_i|Y}, p_{\hat{X}_i|Y})) \\
&= nR_C^I(\mathbb{E}[\Delta(X^n, \hat{X}^n)|Y], d(p_{X|Y}, p_{\hat{X}|Y})) \\
&\stackrel{(d)}{\geq} nR_C^I(D, P),
\end{aligned} \tag{15}$$

where (a) is due to data pre-processing inequality [Cover, 1999], (b) is the definition of $R_C^I(D, P)$, (c) is due to the convexity of $R_C^I(D, P)$ in Theorem 2.1, (d) is due to the monotonicity of $R_C^I(D, P)$ in Theorem 2.1. \square

Theorem 2.4. *Perfect conditional perceptual quality leads to perfect perceptual quality.*

Proof. By definition of divergence, $d(p, q) = 0$ if and only if $p = q$. Therefore, $d(p_{X|Y}, p_{\hat{X}|Y}) = 0$ leads to $p_{X|Y} = p_{\hat{X}|Y}$, which further leads to $\mathbb{E}_{p_Y}[p_{X|Y}] = \mathbb{E}_{p_Y}[p_{\hat{X}|Y}] = p_X = p_{\hat{X}}$. And finally, we have $p_X = p_{\hat{X}}$, which implies perfect perceptual quality. \square

Theorem 2.5. $R_C^I(D, 0) \leq R_C^I(\frac{1}{2}D, \infty)$;

Proof. This proof closely follows the proof of Theorem. 2 by Blau and Michaeli [2019]. Specifically, we first compute the posterior of X given reconstruction \hat{X} :

$$p_{X|\hat{X}, Y} = \frac{p_{\hat{X}|X, Y} p_{X|Y}}{p_{\hat{X}|Y}} \quad (16)$$

Then, we directly add a posterior mapping from \hat{X} to \tilde{X} using the true posterior:

$$p_{\tilde{X}|\hat{X}, Y} = p_{X|\hat{X}, Y} \quad (17)$$

Then it is obvious that the joint distribution is also the same: $p_{\tilde{X}, \hat{X}|Y} = p_{X, \hat{X}|Y}$. And therefore, the marginal distribution is also the same: $p_{\tilde{X}|Y} = p_{X|Y}$. And therefore, the post-processing mapping $p_{\tilde{X}|\hat{X}, Y}$ achieves perfect perceptual quality. Next, we show the MSE distortion of \tilde{X} is bounded:

$$\begin{aligned} \mathbb{E}[||X - \tilde{X}||^2|Y] &= \mathbb{E}[||X||^2|Y] - 2\mathbb{E}[X^T \tilde{X}|Y] + \mathbb{E}[||\tilde{X}||^2|Y] \\ &\stackrel{(a)}{=} 2\mathbb{E}[||X||^2|Y] - 2\mathbb{E}[X^T \tilde{X}|Y] \\ &= 2\mathbb{E}[||X||^2|Y] - 2\mathbb{E}_{p_{\hat{X}|Y}}[\mathbb{E}_{p_{X, \hat{X}|Y}}[X^T \tilde{X}|\hat{X}, Y]|Y] \\ &\stackrel{(b)}{=} 2\mathbb{E}[||X||^2|Y] - 2\mathbb{E}_{p_{\hat{X}|Y}}[||\mathbb{E}_{p_{X|\hat{X}, Y}}[X|\hat{X}, Y]||^2|Y] \\ &\stackrel{(c)}{=} 2\mathbb{E}[||X||^2|Y] - 2\mathbb{E}_{p_{\hat{X}|Y}}[||\hat{X}||^2|Y] \\ &\stackrel{(d)}{=} 2\mathbb{E}[||X - \hat{X}||^2|Y] \end{aligned} \quad (18)$$

where in (a) we use $p_X = p_{\tilde{X}}$, in (b) we use the fact that X, \tilde{X} is conditional independent given \hat{X}, Y , in (c) we use $\hat{X} = \mathbb{E}[X|\hat{X}, Y]$, as $\mathbb{E}[X|\hat{X}, Y]$ is the optimal solution to minimize MSE. And (d) is equivalent to $\mathbb{E}[X^T \hat{X}|Y] = \mathbb{E}[||\hat{X}||^2|Y]$. And this can be shown by

$$\begin{aligned} \mathbb{E}[X^T \hat{X}|Y] &= \mathbb{E}[\mathbb{E}[X^T \hat{X}|\hat{X}, Y]|Y] \\ &\stackrel{(e)}{=} \mathbb{E}[\mathbb{E}[\mathbb{E}[X|\hat{X}, Y]^T \mathbb{E}[\hat{X}|\hat{X}, Y]|\hat{X}, Y]|Y] \\ &\stackrel{(f)}{=} \mathbb{E}[\mathbb{E}[\hat{X}^T \hat{X}|Y]] \\ &= \mathbb{E}[||\hat{X}||^2|Y], \end{aligned} \quad (19)$$

where (e) is due to the fact that X, \hat{X} are conditional independent given \hat{X} and (f) uses $\hat{X} = \mathbb{E}[X|\hat{X}, Y]$, as $\mathbb{E}[X|\hat{X}, Y]$ is the optimal solution to minimize MSE. And this completes the proof. \square

To proof Theorem 2.6, we need the following lemma:

Lemma 2.6.1. *For optimal one-shot codec, we have deterministic decoder $\hat{X} = \mathbb{E}[X|M, Y]$. On the other hand, for any \hat{X} , there exists only one M that decodes into \hat{X} . To conclude, the optimal one-shot decoder is a deterministic invertible mapping from M to \hat{X} .*

Proof. As M^0 is given, the rate is fixed. For any $\hat{X} \neq \mathbb{E}[X|M^0, Y]$, we just replace it by $\mathbb{E}[X|M^0, Y]$. Then obviously, the distortion is lower, and that is paradox to the optimality of codec. Therefore, we must have $\hat{X} = \mathbb{E}[X|M^0, Y]$.

Similarly, assume both M_1^0 and M_2^0 decode into the same \hat{X} . Then obviously the bitrate to distinguish between M_1^0 and M_2^0 is redundant. More specifically, given \hat{X} , the bitrate has $-\log p(M_1^0) - \log p(M_2^0) + \log(p(M_1^0) + p(M_2^0))$ to improve. And this is paradox to the optimality of codec. Therefore, one \hat{X} can only have one corresponding M . \square

Theorem 2.6. *Given an optimal one-shot codec $f^0(\cdot, Y), g_1^0(\cdot, Y)$ with code M^0 , reconstruction \hat{X} and distortion $\mathbb{E}[\Delta(X, \hat{X})|Y] \leq D/2$. there exists an optimal perceptual decoder $g_2(\cdot, Y)$ with $p_{\hat{X}|M^0, Y} = p_{X|M^0, Y}, d(p_{X|Y}, p_{\hat{X}|Y}) = 0, \mathbb{E}[\Delta(X, \hat{X})|Y] \leq D$;*

Proof. To proof Theorem 2.6, we first prove that their exist a decoder with decoding function $p_{\hat{X}|M^0, Y} = p_{X|M^0, Y}$, perfect perceptual quality $d(p_{X|Y}, p_{\hat{X}|Y}) = 0$, and distortion $\mathbb{E}[\Delta(X, \hat{X})|Y] \leq D$.

As Lemma 2.6.1 tells us that \hat{X} and M are deterministic invertible mapping, then we have $p_{X|M, Y} = p_{X|\hat{X}, Y}$ and $p_{\hat{X}|M, Y} = p_{\hat{X}|\hat{X}, Y}$. And the rest of proof follows the proof of Theorem 2.5. Similar trick can also provide an alternative proof of Theorem. 2 in Yan et al. [2021], which is the non-conditional version of Theorem 2.6.

Next, we prove the optimality of such decoder. Consider for each $y \in \mathcal{Y}$, we iteratively apply Theorem. 1 of Yan et al. [2021] and construct $|\mathcal{Y}|$ decoders. According to Yan et al. [2021], those decoders are optimal for each y and satisfies $p_{X|M, Y=y} = p_{X|\hat{X}, Y=y}$. Next, let's construct a meta-decoder by combining those optimal decoders, and we notice that the distortion and perception are satisfied. Furthermore, we have $p_{X|M, Y} = p_{X|\hat{X}, Y}$. And such meta-decoder is a valid solution to the constrains. We notice that the rate of this decoder is a linear combination of rate for each y . Let's assume another codec with rate less than this rate exists, then for at least one of $y \in \mathcal{Y}$, the rate of this codec is less than the optimal rate by Theorem. 1 of Yan et al. [2021]. And this brings paradox. Thus, no other codec satisfying the distortion perception constrains has strictly less rate than the meta-decoder. And we can say the meta-decoder with $p_{X|M, Y} = p_{X|\hat{X}, Y}$ is optimal. \square

Theorem 3. *Assume $d(p_{X|Y}, p_{\hat{X}|Y}) = 0$ and Y is deterministic of X , for any codec with total expected code length R and code M , there exists another codec that has the same code M following the above framework with Y encoded losslessly, whose total expected code length $R_M + R_Y \leq R + 2$.*

Proof. Denote the encoder of first codec as $f(\cdot, Y)$, and the code as $M = f(X, Y)$. For the second codec, we do not change encoder or decoder. Instead, as both the encoder and decoder has Y before we encode and decode M , we encode M with conditional entropy model with entropy $H(M|Y)$. And the total entropy for the second codec is:

$$\begin{aligned} H(M, Y) &= H(M|Y) + H(Y) \\ &= H(M) + H(Y|M) \end{aligned} \tag{20}$$

We note that the first line of Eq. 20 is the entropy of the second codec, and the second line is the entropy of first codec plus an overhead $H(Y|M)$. Next, we examine this overhead $H(Y|M)$:

$$\begin{aligned} H(Y|M) &\stackrel{(a)}{\leq} H(Y|\hat{X}) \\ &\stackrel{(b)}{=} H(Y|X) \\ &\stackrel{(c)}{=} 0 \end{aligned} \tag{21}$$

where in (a) we use data processing inequality [Cover, 1999], in (b) we use the assumption that $d(p_{X|Y}, p_{X|\hat{Y}}) = 0$ and in (c) we use the assumption that Y is deterministic of X . Therefore, we have $H(M|Y) + H(Y) = H(M)$.

From Kraft's inequality [Cover, 1999]. , we have:

$$\begin{aligned} H(Y) &\leq R_Y \leq H(Y) + 1 \\ H(M|Y) &\leq R_M \leq H(M|Y) + 1 \\ H(M) &\leq R \leq H(M) + 1 \end{aligned} \tag{22}$$

Therefore, we have:

$$\begin{aligned} R_Y + R_M &\leq H(Y) + H(M|Y) + 2 \\ &\stackrel{(d)}{=} H(M) + 2 \\ &\leq R + 2 \end{aligned} \tag{23}$$

, where (d) use previous result that $H(Y|M) = 0$. And this completes the proof. \square

Theorem 4. *For one-shot codec, to achieve perfect perceptual quality at rate R^0 , we require a common randomness $W \in \mathcal{W}$ with $\log |\mathcal{W}| \geq H(W) \geq H(X) - (R^0 + 1)$. To achieve perfect conditional perceptual quality, we require $\log |\mathcal{W}| \geq H(W) \geq H(X|Y) - (R^0 + 1)$.*

Proof. Let's first consider the perfect perceptual quality case. Consider a one-shot codec encoding image X into bitstream M , and reconstructs \hat{X} , we have:

$$\begin{aligned} H(\hat{X}, M) &= H(\hat{X}|M) + H(M) \\ &= H(\hat{X}) + H(M|\hat{X}) \\ &\geq H(\hat{X}) \\ &\stackrel{(a)}{=} H(X), \end{aligned} \tag{24}$$

where (a) is due to $d(p_X, p_{\hat{X}}) = 0$. And this leads to:

$$\begin{aligned} H(\hat{X}|M) &\geq H(X) - H(M) \\ &\stackrel{(b)}{>} H(X) - (R^0 + 1), \end{aligned} \tag{25}$$

where (b) is due to Kraft inequality [Cover, 1999]. For lossy compression, as $H(\hat{X}|M) > 0$, we need a stochastic decoder. Specifically, given code M , the decoder has a reconstruction \hat{X} whose conditional entropy is at least $H(\hat{X}|M)$. When decoder is a conditional GAN, this means that the noise W 's entropy is at least $H(\hat{X}|M)$. To achieve this, we consider a randomness $W \in \mathcal{W}$ shared by encoder and decoder, which is independent of M . With W , we require \hat{X} to be deterministic, otherwise the encoder side has no idea of what the decoder side reconstruction \hat{X} looks like. The coding procedure resembles the bits-back coding [Townsend et al., 2018]. When encoding, we first sample \hat{X} from $p(\hat{X}|M)$ with an expected bitrate $H(\hat{X}|M)$. And this requires W has a entropy of $H(\hat{X}|M)$. As the alphabet size of W , $|\mathcal{W}|$ is at least $2^{H(W)}$, we need an alphabet size $|\mathcal{W}|$ of at least $2^{H(\hat{X}|M)}$. During decoding, we also sample \hat{X} from $p(\hat{X}|M)$ from the very same W . More specifically:

$$\begin{aligned} H(\hat{X}|W, M) &= 0 \\ &= H(\hat{X}|M) - H(W|M) \\ &\stackrel{(c)}{=} H(\hat{X}|M) - H(W), \end{aligned} \tag{26}$$

where (c) is due to the fact that $W \perp M$. And from Theorem 2.6.4 of Cover [1999], we have

$$\log |\mathcal{W}| \geq H(W) \geq H(X) - (R^0 + 1). \tag{27}$$

Similar proof applies to the conditional perceptual quality case. We only add additional limitation that W is also independent of Y and condition M, \hat{X} on Y , and everything else in the proof remains the same. \square

B More Experimental Results

B.1 More Experiment Setup

For experiment using MNIST dataset [LeCun and Cortes, 2005], we use the default dataset split with 60000 training images and 10000 testing images. All the images are re-scaled into 32×32 and no data augmentation is used. The encoder f , mse decoder g_1 , perceptual decoder g_2 and discriminator h 's architecture follows [Yan et al., 2021]. The optimizer is RMSprop [Hinton et al., 2012]. The learning rate is 10^{-3} for encoder, decoder g_1 , decoder g_2 and 10^{-2} for discriminator h . The model is optimized for 100 epochs with batch-size 128. For the pre-trained classifier, we train a ResNet-18 [He et al., 2015] from scratch using the training dataset. The optimizer we adopt is stochastic gradient descent with momentum [Qian, 1999]. The learning rate is 10^{-2} and the momentum is 0.9. We optimize the model for 10 epochs with batchsize 128. The rate is directly set to $\{4, 8, 12, 16, 20\}$ by forcing the dimension of binary latent code as Yan et al. [2021]. In addition, we also present the detailed neural network architecture in Fig. 8.

| $f(\cdot)$ | $f(\cdot, Y)$ | $H(M Y)$ from $\Pr(M Y)$ |
|---------------------------------|-----------------------------------|--------------------------|
| Conv (1,128,4,2),BN,RELU | Conv (1,128,4,2),BN,RELU | Affine (10,rate-10)+Tanh |
| Conv (128,256,4,2),BN,RELU | Conv (128,256,4,2),BN,RELU | Affine (rate-10,rate-10) |
| Conv (256,512,4,2),BN,RELU | Conv (256,512,4,2),BN,RELU | Categorical Distribution |
| Conv (512,128,4,2),BN,RELU | Conv (512,128,4,2),BN,RELU | |
| Conv (128,rate-10,4,2),Tanh | Conv (128,rate-10,4,2),Tanh | |
| Round(\cdot) | Round(\cdot),Concat Y | |
| $g1(\cdot)$ and $g2(\cdot)$ | $g1(\cdot, Y)$ and $g2(\cdot, Y)$ | |
| DeConv(rate-10,128,4,2),BN,RELU | DeConv(rate,128,4,2),BN,RELU | |
| DeConv(128,512,4,2),BN,RELU | DeConv(128,512,4,2),BN,RELU | |
| DeConv(512,256,4,2),BN,RELU | DeConv(512,256,4,2),BN,RELU | |
| DeConv(256,128,4,2),BN,RELU | DeConv(256,128,4,2),BN,RELU | |
| DeConv(128,1,4,2) | DeConv(128,1,4,2) | |

Figure 8: Detailed neural network architecture used in MNIST dataset. The naming of each components follows Fig. 2. For Conv and Deconv layers, the parameters are input channels, output channels, kernel size and stride. For Affine layers, the parameters are input dimension and output dimensions. The rate parameter differs per bitrate settings. BN is a short for BatchNorm.

For experiment using Cityscape dataset [Cordts et al., 2016], we use the default dataset split with 2975 training images and 500 validation images for test. All the images are re-scaled into 512×256 , and the random horizontal flip is adopted for data augmentation. All the segmentation map is further re-scaled into 64×32 . The encoder f and mse decoder g_1 follow the architecture of Ballé et al. [2018]. The perceptual generator g_2 , discriminator h follow the architecture of Sushko et al. [2020]. We adopt Adam optimizer [Kingma and Ba, 2014]. The learning rate is 4×10^{-3} for discriminator and 10^{-3} for other part of model. We optimize the model for 200 epochs with batchsize 20. The λ trading off rate and distortion is $\{0.00015, 0.0003, 0.0006, 0.00125, 0.0025\}$. The neural network architecture used in this experiment is too complicated to be expanded exactly. Thus, we depicted the architecture in Fig. 9 with modules copied from Ballé et al. [2018], Park et al. [2019]. We refer interested readers those papers or the source code for exact details.

B.2 More Quantitative Results

In Section 4.2 we do not have room to list the bitrate and other metrics for distortion-conditional perception trade-off. In Tab. 3, we provide all the metrics comparing linear interpolation of images and manual adjusting β .

B.3 More Qualitative Results

See more qualitative results for MNIST dataset in Fig. 11-15. See more qualitative results for Cityscape dataset in Fig. 16-Fig. 19.

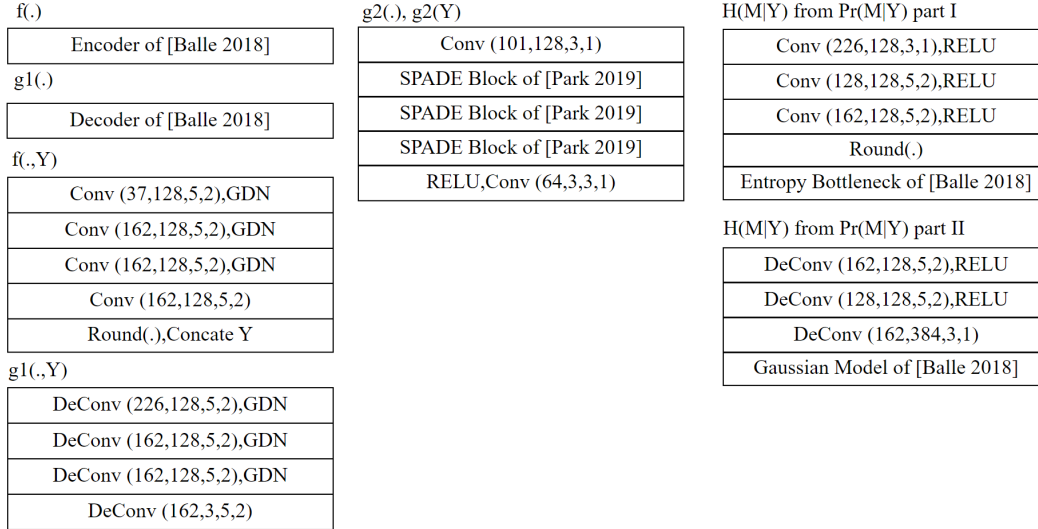


Figure 9: Detailed neural network architecture used in Cityscape dataset. We do not employ different architecture for $g_2(\cdot)$ and $g_2(\cdot, Y)$. Instead, we just set Y to 0 when we want $g_2(\cdot)$.

Table 3: The rate, MSE, conditional FID, FID and accuracy of linear interpolation of images and manual adjusting β .

| | Rate (bits) ↓ | MSE ↓ | ConFID ↓ | FID ↓ | acc ↑ |
|---------------------|---------------|--------|----------|--------|--------|
| Image Interpolation | 4.29 | 0.0821 | 25.55 | 14.33 | 0.9754 |
| | 4.29 | 0.0741 | 27.22 | 15.96 | 0.9778 |
| | 4.29 | 0.0668 | 33.78 | 20.72 | 0.9803 |
| | 4.29 | 0.0553 | 55.07 | 38.15 | 0.9729 |
| | 4.29 | 0.0469 | 89.15 | 65.69 | 0.9518 |
| | 4.29 | 0.0422 | 136.14 | 104.01 | 0.9059 |
| | 4.29 | 0.0405 | 225.54 | 178.80 | 0.8363 |
| β Adjustment | 4.35 | 0.0783 | 39.29 | 25.32 | 0.9758 |
| | 4.30 | 0.0760 | 46.69 | 31.61 | 0.9704 |
| | 4.32 | 0.0598 | 62.66 | 43.68 | 0.9368 |
| | 4.33 | 0.0507 | 82.14 | 57.95 | 0.9569 |
| | 4.26 | 0.0431 | 112.51 | 83.10 | 0.9625 |
| | 4.29 | 0.0405 | 225.54 | 178.80 | 0.8363 |

B.4 Evaluation on Common Randomness Required

We verify the correctness of Theorem 4 by adjusting the amount of common randomness $H(W)$ and observe its impact on perceptual quality. The MNIST dataset is used and the experimental setup is the same as Section. 4.2. We constrain the noise W 's entropy that is injected in g_2 and observe its effect on FID. The $H(X)$ is approximated by the lossless compression rate of MNIST. We directly take the result from [Townsend et al., 2018] and assume that $H(X) \approx 1105.44$ bits.

More specifically, we use fully factorized unit Gaussian noise, which means that $W \sim \mathcal{N}(0, I)$. As the quantization of float32 is uneven, we can not directly obtain entropy $H(W)$ from the differentiate entropy of $\mathcal{N}(0, I)$. Therefore, we manually estimate the $H(W)$ by Monte Carlo. Specifically, we draw sample $w \sim \mathcal{N}(0, 1)$, and find its previous float32 w_{-1} , its next float32 w_{+1} , and approximate its support as $\delta = (w_{+1} - w_{-1})/2$. Next, we estimate the probability mass of w as $p(w) = \text{cdf}_{\mathcal{N}(0,1)}(w + \delta/2) - \text{cdf}_{\mathcal{N}(0,1)}(w - \delta/2)$, and the information as $-\log p(w)$. We repeat this process many times and obtain the average information. According to the weak law of large number [Cover, 1999], this average converges to true entropy. We sample 10^6 times, and obtain an average entropy of 26.55 bits per dimension.

We gradually add noise W to perceptual decoder g_2 from deterministic to $H(W) \geq H(X) - (R^0 + 1)$. The R^0 is the rate of codec, which is set to 4 and 32. As shown in Fig. 10, for low bitrate such as 4 bits, it is quite clear that an insufficient amount of noise entropy $H(W)$ severely affect the perceptual quality (FID 238.77 vs 18.76). However, for high bitrate, even deterministic codec can achieve a high perceptual quality (FID 23.23). And the advantage of perceptual quality for sufficient noise beyond the lowerbound is not as obvious as low bitrate (FID 19.25 vs 23.23). Theoretically, it is necessary to have $H(W) \geq H(X) - (R^0 + 1)$ for perfect perceptual quality. Practically, we can not achieve perfect perceptual quality due to the capacity or optimization of generative model. Therefore, when bitrate is high, the effect of insufficient noise entropy $H(W)$ might not obvious.

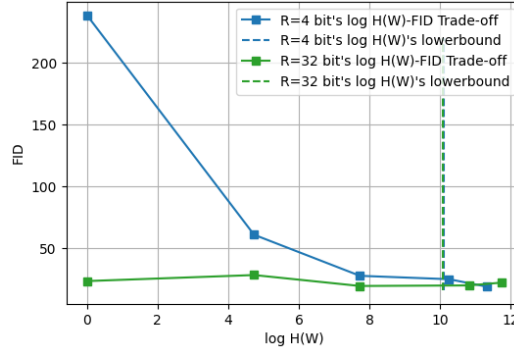


Figure 10: The effect of common randomness on perceptual quality. We define $\log H(W) = 0$ instead of $-\infty$ as deterministic.

C More Discussions

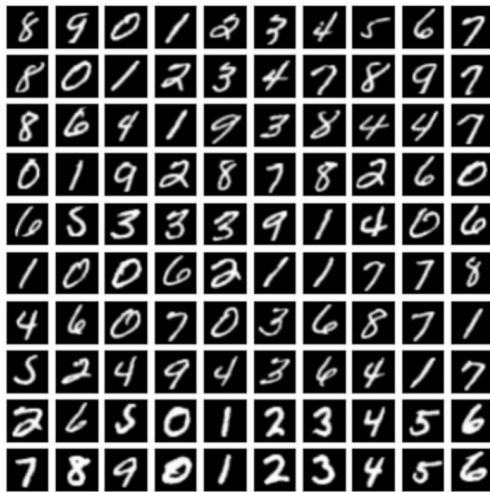
C.1 Broader Impacts

Saving bitrate without harming perceptual quality and semantic information in image has positive social impact. A large amount of energy and resources are spent on the transmission and storage of image data. Reducing the bitrate can save the resources, energy and the carbon emission during the process.

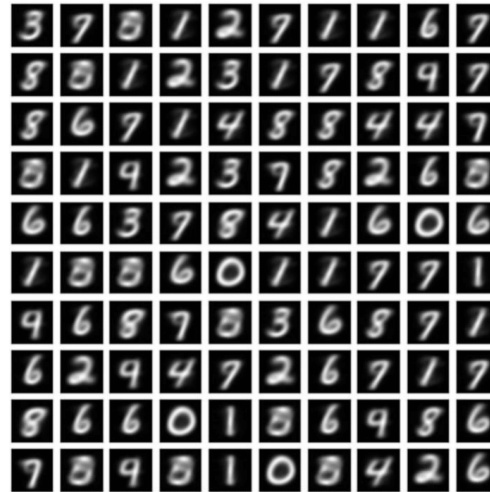
C.2 Reproducibility Statement

All theoretical results are proven in Appendix. A. For experimental results, both MNIST and Cityscape dataset are publicly accessible. We provide implementation details in Appendix. B.1. Furthermore, the source code for reproducing empirical results are provided in supplementary materials.

Original Image



MSE optimized compression
4 bits



Perceptual quality preserving compression
4 bits



Conditional perceptual quality preserving compression
4.2 bits

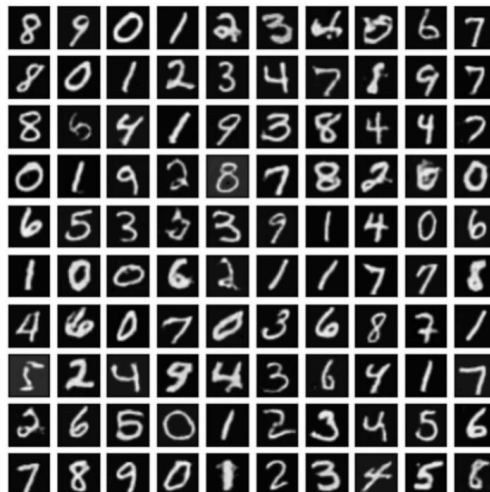
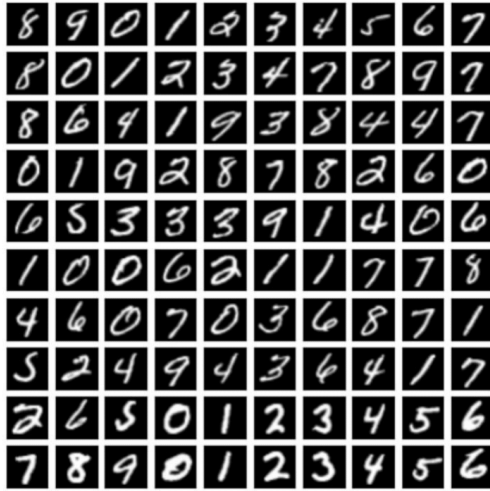


Figure 11: Qualitative results comparing original image, baseline MSE codec, perceptual quality preserving codec [Yan et al., 2021] and our proposed conditional perceptual preserving codec for MNIST dataset with rate ≈ 4 bits.

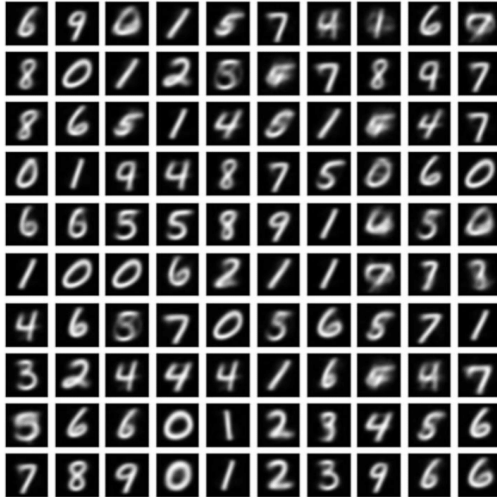
Original Image



MSE optimized compression
8 bits



Perceptual quality preserving compression
8bits



Conditional perceptual quality preserving compression
7.2 bits

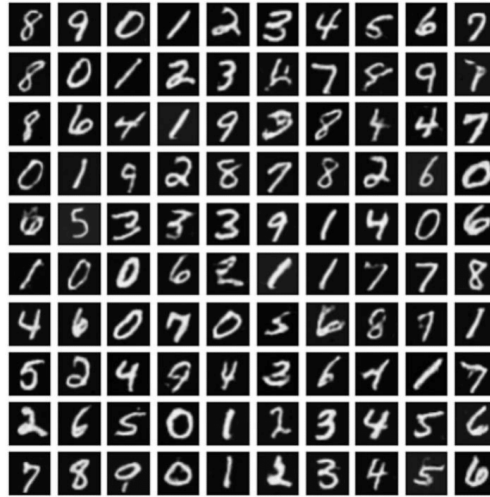
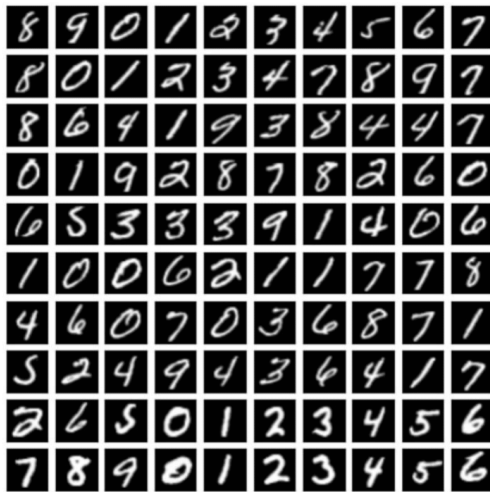
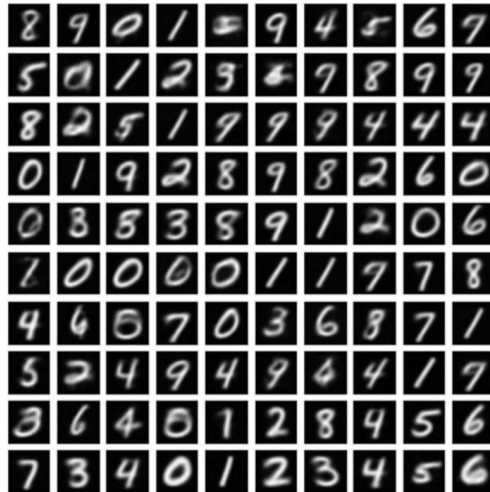


Figure 12: Qualitative results comparing original image, baseline MSE codec, perceptual quality preserving codec [Yan et al., 2021] and our proposed conditional perceptual preserving codec for MNIST dataset with rate ≈ 8 bits.

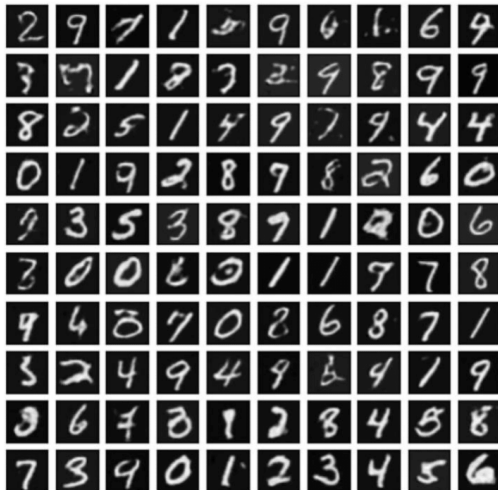
Original Image



MSE optimized compression
12 bits



Perceptual quality preserving compression
12 bits



Conditional perceptual quality preserving compression
11.1 bits

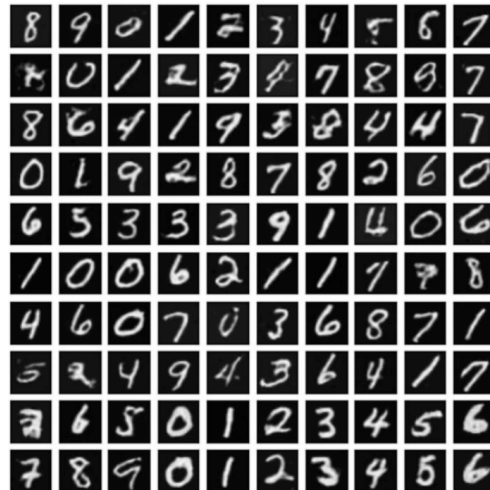
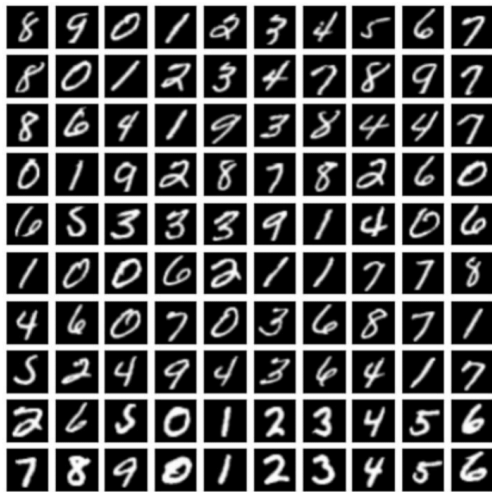
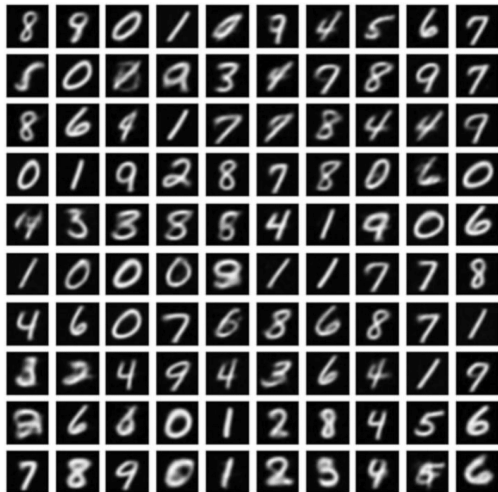


Figure 13: Qualitative results comparing original image, baseline MSE codec, perceptual quality preserving codec [Yan et al., 2021] and our proposed conditional perceptual preserving codec for MNIST dataset with rate ≈ 12 bits.

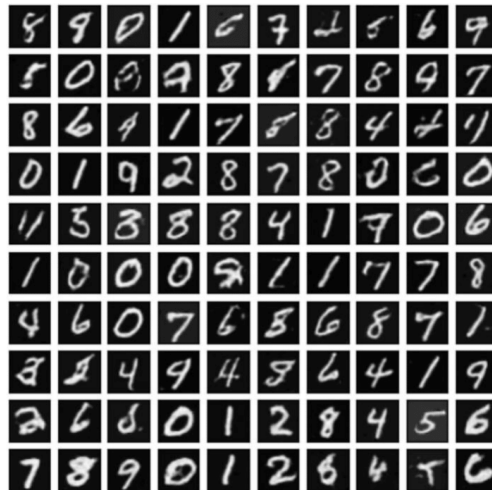
Original Image



MSE optimized compression
16 bits



Perceptual quality preserving compression
16 bits



Conditional perceptual quality preserving compression
15.2 bits

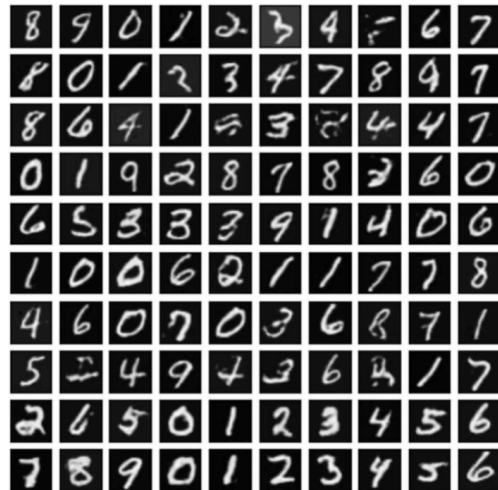
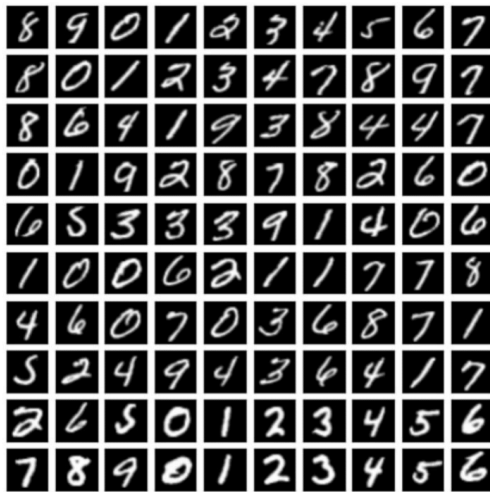
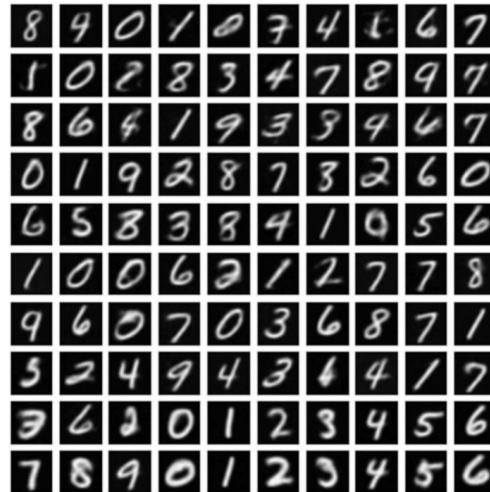


Figure 14: Qualitative results comparing original image, baseline MSE codec, perceptual quality preserving codec [Yan et al., 2021] and our proposed conditional perceptual preserving codec for MNIST dataset with rate ≈ 16 bits.

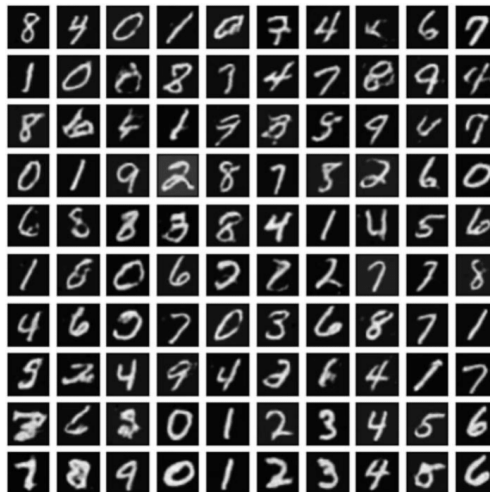
Original Image



MSE optimized compression
20 bits



Perceptual quality preserving compression
20 bits



Conditional perceptual quality preserving compression
19.0 bits

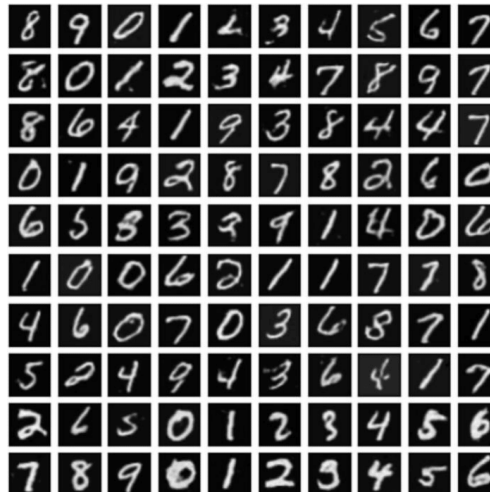
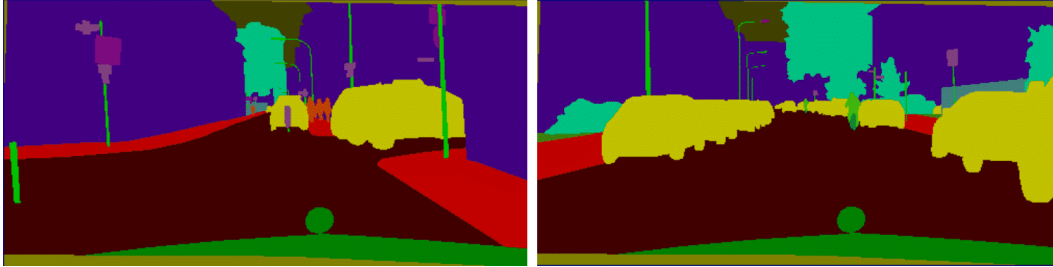


Figure 15: Qualitative results comparing original image, baseline MSE codec, perceptual quality preserving codec [Yan et al., 2021] and our proposed conditional perceptual preserving codec for MNIST dataset with rate ≈ 20 bits.

Original Image



Segmentation map



MSE optimized compression
0.0203 bpp



Perceptual quality preserving compression
0.0203 bpp



Conditional perceptual quality preserving compression
0.0183 bpp

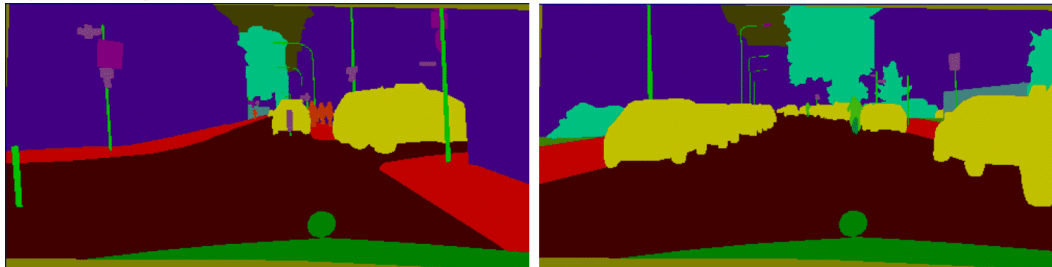


Figure 16: Qualitative results comparing original image, baseline MSE codec, perceptual quality preserving codec [Yan et al., 2021] and our proposed conditional perceptual preserving codec for Cityscape dataset with rate ≈ 0.02 bpp.

Original Image



Segmentation map



MSE optimized compression
0.0350 bpp



Perceptual quality preserving compression
0.0350 bpp



Conditional perceptual quality preserving compression
0.0410 bpp

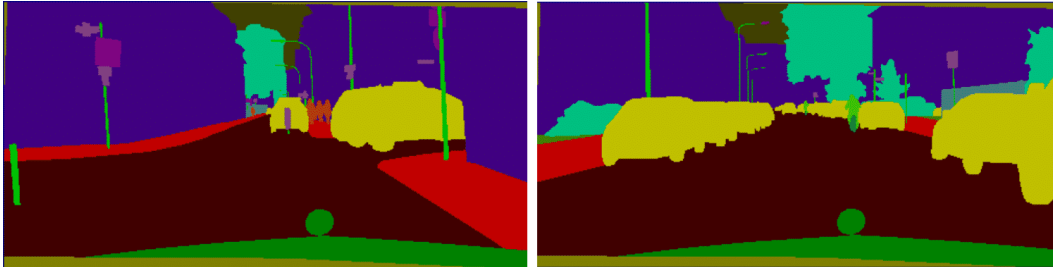


Figure 17: Qualitative results comparing original image, baseline MSE codec, perceptual quality preserving codec [Yan et al., 2021] and our proposed conditional perceptual preserving codec for Cityscape dataset with rate ≈ 0.04 bpp.

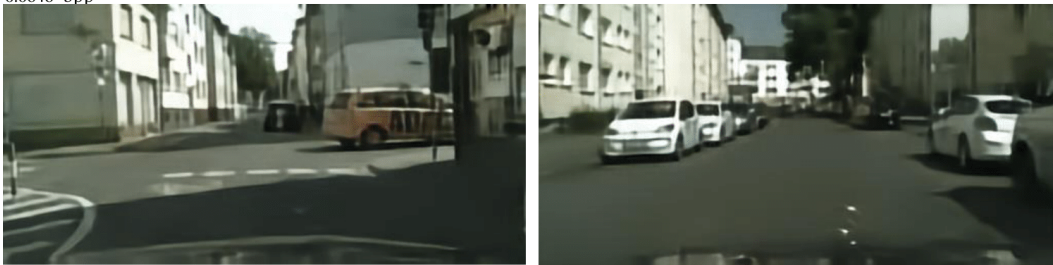
Original Image



Segmentation map



MSE optimized compression
0.0646 bpp



Perceptual quality preserving compression
0.0646 bpp



Conditional perceptual quality preserving compression
0.0698 bpp

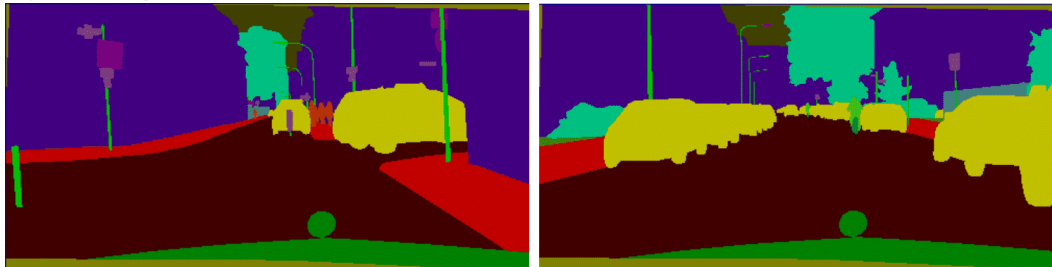


Figure 18: Qualitative results comparing original image, baseline MSE codec, perceptual quality preserving codec [Yan et al., 2021] and our proposed conditional perceptual preserving codec for Cityscape dataset with rate ≈ 0.06 bpp.

Original Image



Segmentation map



MSE optimized compression
0.1108 bpp



Perceptual quality preserving compression
0.1108 bpp



Conditional perceptual quality preserving compression
0.1160 bpp



Figure 19: Qualitative results comparing original image, baseline MSE codec, perceptual quality preserving codec [Yan et al., 2021] and our proposed conditional perceptual preserving codec for Cityscape dataset with rate ≈ 0.1 bpp.